ELSEVIER

Journal of Power Sources 52 (1994) 141–147

JOURNAL OF POWER SOURCES

Short Communication

Performance analysis of photovoltaic-powered water-pumping systems using switched reluctance motor drives

Hamid M.B. Metwally[a,*], Wagdy R. Anis[b]

[a]*Electrical Engineering Department, Faculty of Engineering, Zagazig University, Zagazig, Egypt*

[b]*Electronics and Communications Department, Faculty of Engineering, Ain Shams University, 1 Sarayat Street, Abbasia, Cairo, Egypt*

Received 16 May 1994, accepted 9 June 1994

Abstract

A photovoltaic-powered (PV) pumping system that uses a switched reluctance motor (SRM) is investigated. The motor is supplied by a d.c. voltage through a switching circuit. The drive circuit is much simpler than the normal d.c./a.c inverter that is required to supply the induction motor. The efficiency of the SRM is considerably higher than that of equivalent d.c. or induction motors. In addition, because of the simple construction, the SRM is cheaper. By virtue of these advantages of the SRM, the proposed system has higher efficiency and lower cost compared with other systems. A design example is studied in detail to explore the advantages of PV pumping systems based on this new drive. It is found that the operating efficiency of the motor is about 85% during most of its working time. The matching efficiency between the PV array and the proposed system approaches 95%. The major part of the losses takes place in the pump and the riser pipes; this loss represents one-third of the total available energy.

Keywords Pumping systems; Photovoltaic array system

1. Introduction

Water pumping is one of the most popular applications of solar energy. A pumping system consists of three basic components, namely, a photovoltaic (PV) array, an electric motor, and a water pump. In addition, in some cases, there are storage batteries and power-conditioning equipment. To date, either an induction motor or a d.c. motor has been used in these systems.

The squirrel-cage induction motor is a well-developed and reliable device. It is one of the simplest forms of the available motors. Because of its simplicity, it is cheap, robust, and has low-maintenance requirements. An electronic inverter is necessary to convert the d.c. power generated by the array to a.c. power for the motor. For variable speed operation, a variable frequency supply is required. The supply must also be of variable voltage if a constant torque is to be obtained throughout the speed range. The requirements of variable voltage and frequency supply, as well as an a.c. waveform with minimal harmonics, necessitate the use of a complex and hence expensive inverter. As the inverter becomes complex, the reliability in service decreases.

The d.c. motor, on the other hand, is more complicated and, therefore, is more expensive. It has all the common disadvantages associated with the sliding brush contacts and commutator, such as the need for routine inspection and periodic maintenance. Brush contacts are also unsuitable for hazardous environments and the associated arcing problem limits both the size and the speed range of the motor. Direct current motors are not suitable for high speeds because of the wear and tear of the commutator and brushes which shorten the operational life. In spite of all these disadvantages, d.c. motors are used extensively in PV pumping systems. This is because they can be coupled directly to the PV array giving a simple and inexpensive system. The design and performance of directly-coupled PV pumping systems have been investigated in many publications [1–4].

In order to avoid the complex electronic inverter needed for the induction motor and the brush/commutator problem in conventional d.c. motors, brushless

*Corresponding author. Yanbu Industrial College, PO Box 30436, Yanbu Al Sinaiyah 21477, Saudi Arabia

SSDI 0378-7753(94)01946-S

d.c. motors are used in pumping systems, but only to a limited extent. The brushless d.c. motor has a rotating permanent magnet and a stationary armature winding and thus avoids brushes and a commutator. Commutation of electric current in the stationary armature is achieved by an electronic circuit in accordance with the rotor position. This is why brushless d.c. motors are called electronically commutated d.c. motors. The design of a PV pumping system based on this drive has been reported previously [5].

In this work, a PV pumping system based on a new drive is investigated. The new drive is called a switched reluctance motor (SRM). Although this motor is a new entrant to the field of variable speed drives, it has gained acceptance worldwide in many general industrial and domestic applications such as fans, blowers, conveyors, and pumps [6]. It may earn the title of the motor of the 1990s.

2. Switched reluctance motor

Recently, the interest in using SRMs as variable speed drives has increased remarkably. This is because this motor has many advantages over other types of motors. It is robust, reliable, cheap, and of higher efficiency. During the last fifteen years or so, many publications concerning the design and performance prediction of this motor have appeared [7,8]. Davis et al. [9] have studied the drive-circuit design, and Finch et al. [10] have investigated the effect of the number of teeth per pole on the performance of the motor.

A brief review of the construction, principle of operation, and figures-of-merit of this motor is given here. Fig. 1 presents the lamination profile of an 8/6 slotted motor as an example. The elementary drive-circuit of one phase is also shown for the purpose of illustration. The construction of the motor is very simple and has the following features:

- salient poles (teeth) on both stator and rotor, i.e., it is doubly salient
- concentrated simple windings mounted on the stator poles
- no windings of any type on the rotor
- the number of poles (teeth) carried on the stator and the rotor are different
- the windings on diametrically opposed poles are connected in series and/or parallel to form one phase, and the number of phases and poles are open to a wide variety of choices

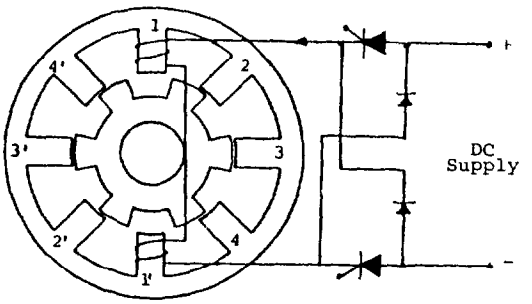

Fig. 1. Cross section of an 8/6 slotted SRM with simplified drive circuit for one phase.

The operation of this motor is based on the production of reluctance torque, that is the torque produced by the forces that tend to align stator and rotor teeth when a particular phase is excited. These forces are independent of the direction of the excitation current. By switching the excitation current between phases, in an appropriate manner, continuous rotation is achieved. The motor may operate in the open-loop or the closed-loop mode of operation. In the open-loop mode, it is not necessary to sense the rotor angle at the instant of switching on and the rotor adjusts itself according to the mechanical load imposed on it. In the closed-loop mode, the phase switching can be controlled via a simple shaft-mounted position transducer, so that the stator windings are switched on and off in accordance with the rotor position.

Simplicity of the construction makes the motor cheap, robust, and reliable. Uni-directional currents in stator windings allow the use of cheap and simple power converters. In addition, this motor has better thermal characteristics than other types of motors because of the absence of windings on the rotor. The above features produce a motor with high specific output and high efficiency over a wide range of speeds and output powers.

3. System model

The block diagram of the system is shown in Fig. 2. It consists of a PV array, a storage battery connected to the array through a battery voltage regulator, a switched reluctance motor together with its drive circuit, and a centrifugal pump. In the following subsections, each component is introduced and the mathematical models for the main components are given.

3.1. PV array

The PV array current/voltage characteristic is given by:

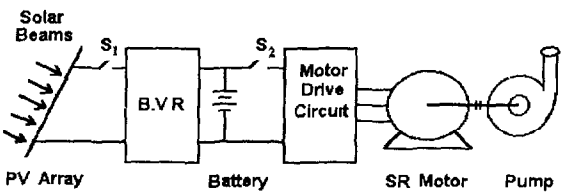

Fig. 2 Block diagram of pumping system.

$$I = I_{L0}G - I_0[\exp((V+IR_S)/V_T) - 1] - (V+IR_S)/R_{Sh} \quad (1)$$

where I is the PV array current (A), I_{L0} the light-generated current of the PV array at $G = 1$ kW m^{-2}, G the solar irradiance (kW m^{-2}), I_0 the PV array reverse saturation current (A), V the PV array operating voltage (V), V_T the thermal voltage of the PV array (V), R_S the series resistance of the PV array (Ω), and R_{Sh} the shunt resistance of the PV array (Ω).

3.2. Battery voltage regulator

The function of the battery voltage regulator (BVR) is to protect the battery against overcharging and deep discharging. If the battery is overcharged, the BVR disconnects the PV array and the load is supplied from the battery. Hence, the battery is partially discharged. On the other hand, if the battery is deeply discharged, the load is disconnected to allow the PV array to charge it. Thus, the BVR controls the battery charge and, consequently, the battery voltage within the allowed limits. Such controlled performance ensures long life for the battery. The detailed design and performance characteristics of one such battery voltage regulator have been given by Anis [11].

3.3. Battery

In some PV systems, a lead/acid storage battery is connected across the PV array through a battery voltage regulator, as shown in Fig. 2. Storage batteries are used in these systems for the following reasons:

- to control the operating voltage of the system so that it is as close as possible to that of the maximum power points of the array and, hence, minimize the array size
- to minimize load voltage variations
- to store excess energy during high insolation periods in order for the system to be used during low insolation periods; this allows maximum utilization of the available solar energy
- to supply impulsive load current, if needed.

In addition, for the type of drive considered in this work (SRM), it has been found that there is an optimum operating d.c. voltage for each given speed and load torque, as reported by Metwally [12]. Hence, by proper choice of the battery voltage, an optimum operation of the motor can be achieved. Direct coupling of the PV array to SRM driving a pump requires a sophisticated drive circuit to allow for the changes in voltage by changing the speed of the motor to guarantee maximum utilization of the available solar energy. Future work will consider a directly-coupled pumping system using SRM drive.

3.4. Drive circuit

The switched reluctance motor operates well from a switched voltage supply. Unlike conventional motors, a square-wave of voltage is a better excitation waveform than a sine wave. This is because the square-wave voltage helps to build up the phase current quickly and, hence, produces more torque. The general shape of this voltage waveform is shown in Fig. 3. The voltage is switched on at instant t_1 and off at instant t_2; the negative voltage is used for commutation. Hence, the drive circuit is simple, and its main task is to switch the voltage on and off in an appropriate way. Many drive-circuit configurations are possible. Fig. 1 shows a schematic for the most common one. There are two main power switches per phase, only the circuit for one phase is shown in this diagram. Power is drawn from the supply when the two switches are turned on, and is returned to it when the switches are turned off. Thus, the commutation power is returned to the supply instead of being wasted in the freewheeling resistance, as is the case in the induction motor. This increases the efficiency of the motor.

3.5. Switched reluctance motor

The mathematical model of the switched reluctance motor consists of the electrical and mechanical equations that govern its behaviour under given operating conditions. In general, there is one voltage equation for each phase of the motor. In addition, there are two mechanical equations that represent the motor dynamics. Assuming an n-phase motor, then the mathematical model is given by the following $(n+2)$ equations:

$$V_j = i_j R_j + \frac{d\Psi_j}{dt} \quad (2)$$

$$\frac{d\theta}{dt} = \omega \quad (3)$$

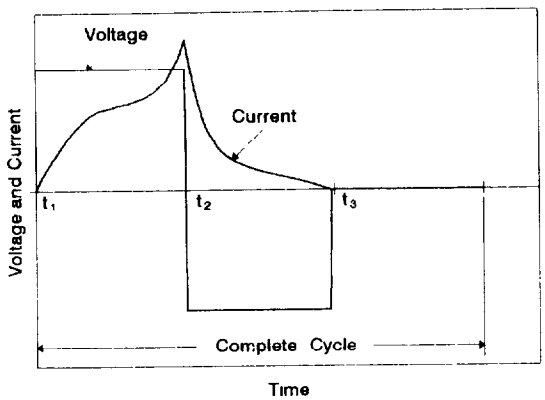

Fig. 3 Typical voltage and current waveforms of switched reluctance motors.

$$\frac{d\omega}{dt} = \frac{1}{J}(T - T_m) \tag{4}$$

where j represents the phase number, V is the phase applied voltage (V), i the phase current (A), R the phase resistance (Ω), Ψ the phase flux-linkage (wb-turn), θ the rotor angle in mechanical radians, ω the rotor speed (rad s^{-1}), J the rotor and load moment of inertia (Nm s^2), T the electromagnetic torque developed by motor (Nm), and T_m the mechanical load torque, including the effects of motor and load friction.

The flux-linkage function, Ψ, given in the above equations depends on both the rotor angle, θ, and the phase current, i, in a complicated nonlinear manner and is usually written in the form $\Psi(\theta, i)$. In order to solve the motor model, the function $\Psi(\theta, i)$ must be known: either in an analytical form or in the form of tabulated measured data. Once this function is known, the electromagnetic torque developed by the motor can be calculated using the co-energy function as follows:

$$W'(\theta, i) = \int_0^i \Psi(\theta, i)\,di \Big|_{\theta = \text{constant}} \tag{5}$$

and,

$$T(\theta, i) = \frac{\partial W'}{\partial \theta}\Big|_{i = \text{constant}} \tag{6}$$

where $W'(\theta, i)$ is the co-energy function, and $T(\theta, i)$ the electromagnetic torque function.

The $(n+2)$ Eqs. (2) to (4), together with the flux-linkage function $\Psi(\theta, i)$ and the static torque Eqs. (5) and (6), represent the complete mathematical model of the n-phase switched reluctance motor. The following assumptions are made to obtain the steady-state performance: (i) all motor phases are symmetrical; (ii) the mutual flux-linkage between phases is small enough to be neglected, and (iii) the motor is running at constant speed.

The above assumptions reduce the model of the motor to one voltage equation in the following form:

$$\frac{d\Psi}{dt} = V - iR \tag{7}$$

By differentiating the function $\Psi(\theta, i)$ partially with respect to θ and i, Eq. (7) takes the following form:

$$\frac{di}{dt} = \frac{1}{\partial\Psi/\partial i}\left(V - iR - \omega\frac{\partial\Psi}{\partial\theta}\right) \tag{8}$$

It should be noted here that, although the model is a steady-state one, it contains a differential equation. This is because all the parameters of the motor are time-dependent and not constant, as is the case with a d.c. motor. In order to solve this model, the function $\Psi(\theta, i)$ must be obtained either experimentally or by using the finite-element method. The solution of Eq. (8) for a given voltage waveform produces the motor phase current i, as a function of time, t, and hence the torque produced by the motor can be calculated by using Eqs. (5) and (6). Eq. (8) may be solved using the well-known Runge–Kutta fourth order method for solving differential equations.

3.6. Pump

Braunstein and Kornfeld [3] have reported that the torque required to drive the centrifugal pump is given by:

$$T_p = K_p\omega^2 \tag{9}$$

where T_p is the torque required to drive the pump (Nm), and K_p is constant for a given pump.

4. Design example

In the following discussion, detailed calculations of an illustrative design example are given. It is assumed that it is required to pump water from a depth of 28 m at a rate of 150 m^3/day. This amount of water is sufficient to irrigate a vegetable farm with an area of two acres.

4.1. Pump

Assuming that the PV pumping system operates for 10 h each day, then the required discharge, Q, is $Q = 4.167 \times 10^{-3}$ m^3 s^{-1}. The relationship between the diameter of the riser pipe, D, and the speed of water v, is given by the continuity equation:

$$Q = \frac{\pi D^2 v}{4} \tag{10}$$

If a 2 inch diameter riser pipe is used, then from Eq. (10), the water speed, v, is equal to 2.056 m s^{-1}. From the friction charts given by Karassik et al. [13] and considering a smooth pipe, the friction factor, f is estimated to be $f = 0.018$. The friction head, H_f, is given by:

$$H_f = \frac{fLv^2}{2Dg} \tag{11}$$

where L is the length of the riser pipe (m), 28 m in this example; g is the gravitational acceleration (m s^2). Substituting in Eq. (11), gives $H_f = 2.127$ m. Hence, the total required head, H, is approximately equal to 30 m.

From the above analysis, it can be concluded that a pump delivering 15 m^3 per h at a head of 30 m is required. The commercial, four-stage centrifugal pump

whose H/Q characteristic is shown in Fig. 4 is chosen. It delivers about 16.5 $m^3 h^{-1}$ at 30 m head when driven at 1350 rpm. At this operating point, the mechanical power input to the pump is 3 hp, hence the torque required to drive the pump is $T_p = 15.83$ Nm, and the efficiency of the pump is 56.3%.

4.2. Motor

The motor used in this example is a 3 kW, three-phase, switched reluctance motor. The measured flux-linkage/phase-current/rotor-angle characteristics of the motor are available from a previous work by Metwally [12]. Using the mathematical model of the motor, its performance curves are calculated and are shown in Figs. 5 and 6. Fig. 5 gives the torque/speed characteristics at different d.c. voltages. Fig. 6 indicates the corresponding d.c. current/speed characteristics. Since the operating point of the pump is 15.83 Nm at 1350 rpm, the d.c. voltage required to drive the motor must be at least 84 V. Fig. 7 shows that the current drawn by the motor varies between 29 and 26 A (points C and D) according to the variations of the battery voltage.

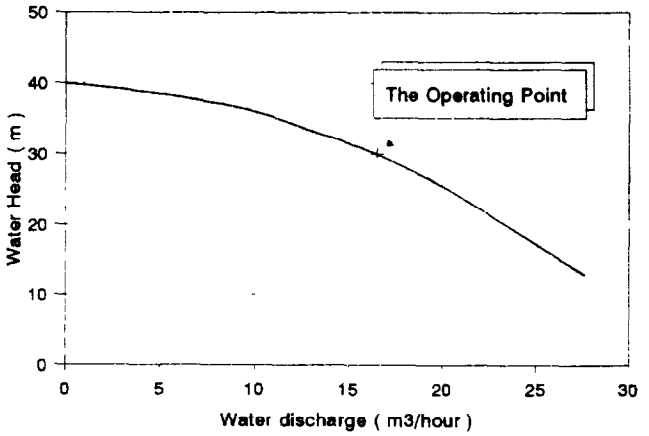

Fig. 4. Water head/water discharge characteristics of pump at 1350 rpm.

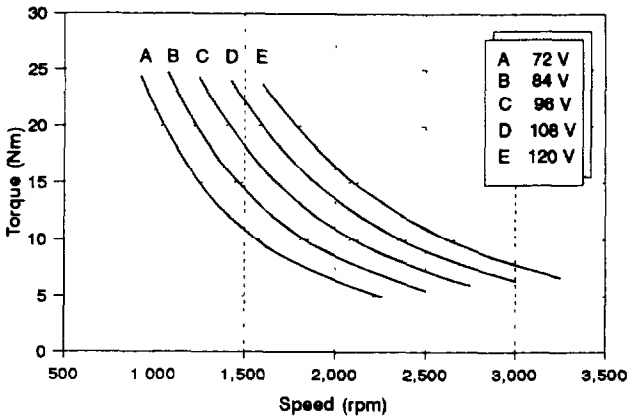

Fig. 5. Torque/speed/d.c. voltage characteristics of switched reluctance motor.

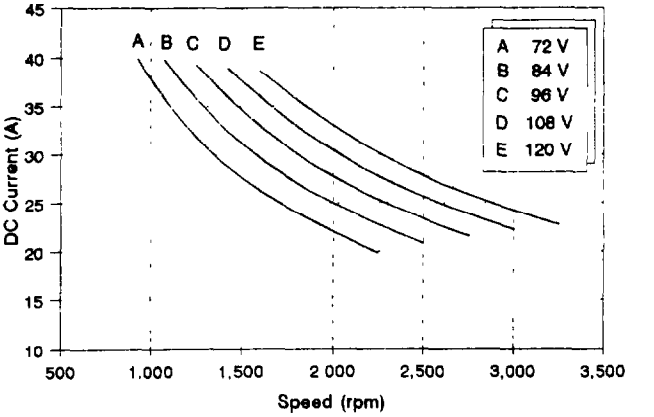

Fig. 6. D.c. current/speed/d c. voltage characteristics of switched reluctance motor.

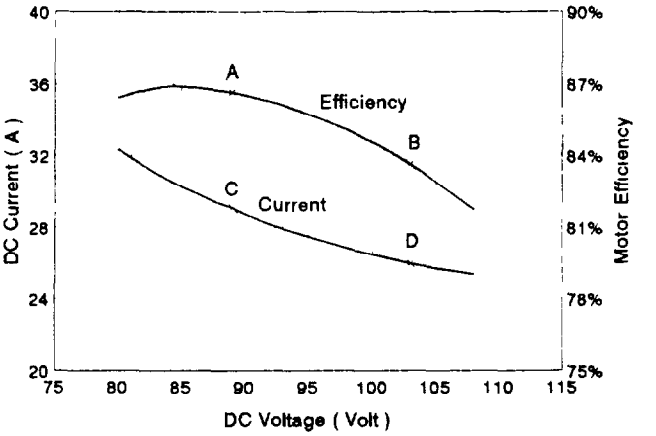

Fig. 7. Variations of d.c. current and efficiency with d.c. voltage, at 1350 rpm and 15.83 Nm.

Also, the efficiency of the motor lies between 86.7 and 83.6% (points A and B), but it is above 85% for most of the time.

4.3. Battery and voltage regulator

Since the voltage required to drive the motor is at least 84 V, the nominal voltage of the battery is taken as 96 V. During the winter solistice day, the voltage will change according to the state-of-charge of the battery between a minimum value of 88.8 V and a maximum value of 103 V, as can be seen from Fig. 7. Accordingly, the current required to drive the motor at 1350 rpm and 15.83 Nm will vary between 29 and 26 A. The BVR controls the voltage between the above limits, according to the state-of-charge of the battery as explained earlier.

4.4. PV array

To calculate the size of the PV array the following assumptions are made:

(i) climatic conditions of Cairo city (30° N) are considered;

(ii) water discharge is guaranteed for sunny days only, thus it may be interrupted during cloudy days;

(iii) according to Cairo climatic conditions, cloudy days take place only a few times during the winter when water demand is minimum; hence, the system guarantees water supply almost throughout the whole year;

(iv) the PV array tilt angle is 45° and facing south;

(v) the battery voltage is controlled by a conventional regulator;

(vi) the effect of ambient temperature variations on the PV array performance is considered, and

(vii) the minimum allowed state-of-charge of the battery is 25%.

A detailed simulation programme has been developed to determine the PV array and the battery storage sizes. Using this programme, the following results are obtained; (i) PV array size is 6.048 kW peak, and (ii) battery capacity is 1060 Ah.

The proposed system operates 12 h each day for most of the year. During spring, summer and autumn, the system delivers 180 m^3 of water per day. Winter is the exceptional season when the system delivers 150 m^3 per day. Thus, the annual average discharge exceeds 170 m^3 per day.

5. System performance

The maximum and utilized power of the array during the winter solistice day are given in Fig. 8. It is obvious that the utilized power is slightly less than the maximum power, the difference represents the mis-match loss. It can be seen that the utilized power has two abrupt changes at points E and F. At point E, the state of the battery changes from discharge to charge and, as a result, its voltage rises abruptly and leads to a better match with the PV array. Conversely, at point F, the battery state changes from charge to the discharge and, hence, its voltage drops suddenly and causes a poor match with the PV array. Points E and F represent the moments when the utilized array power is just equal to the load power. Fig. 8 also shows variations in battery power during the winter solistice day. The battery power is considered positive during the discharge time, and vice versa.

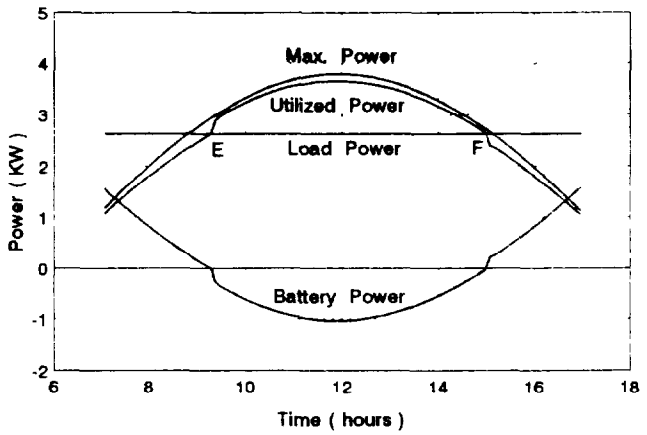

Fig. 8. Variations of different powers during winter solistice day (21 December).

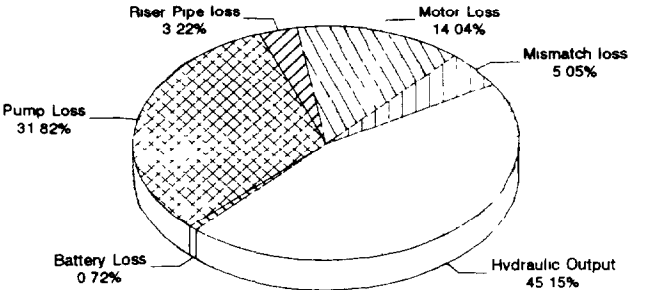

Fig. 9. Distribution of energy during winter solistice day (21 December).

Energy distribution during the winter solistice day is given in Fig. 9. The maximum energy available from the array is considered to be 100%. The mis-match loss is about 5%, and hence the utilized energy is 95% of the maximum available energy. The motor loss is almost 14% of the total energy, this low loss is attributed to the high efficiency of the SRM drive. The largest part of the losses takes place in the pump because of its limited efficiency (about 56%). The useful hydraulic output of the system is 45.15% of the total available array energy. This is significantly higher than that obtainable from systems that use conventional motors. Since the pump loss represents a major part of the total loss of the system, the choice of a more efficient pump, even if it is more expensive, is an effective way to improve the overall efficiency of the system.

6. Conclusions

The steady-state performance of a PV pumping system that employs switched reluctance drive is analysed. This new drive has a number of adavantages over the conventional d.c. and induction drives. High-efficiency and low-maintenance requirements are among the advantages. A mathematical model for each component of the system is introduced. The prediction of SRM performance is quite difficult because of the highly nonlinear

nature of the motor, and also due to the fact that the motor normally operates at high levels of saturation. Thus, the model of the motor has to be solved separately to produce the motor-performance curves. Then, the operating point can be obtained by combining the characteristics of the motor and the pump.

A numerical example is given to illustrate the design procedure. Starting from the required head and discharge, the rating of each component is calculated and a suitable component is chosen. Finally, the sizes of the storage battery and the PV array are calculated.

It has been found that the voltage of the battery varies according to the state-of-charge, but this will not affect the speed of the motor. This is because the speed of a given SRM is determined only by the frequency of the drive circuit. The motor compensates for changes in battery voltage by changing the switch-on angle, but its speed and torque will remain constant. This affects, to some extent, its efficiency. The overall efficiency of the system is found to be above 45%. The level is higher than that of the other systems based on d.c. or induction motors. Further improvement in the efficiency of the system is still possible by choosing a more efficient pump.

References

[1] J. Appelbaum and J. Bany, *Sol Energy, 22* (1979) 439.

[2] J.A. Roger, *Sol. Energy, 23* (1979) 193.

[3] A. Braunstein and A. Kornfeld, *Sol Energy, 27* (1981) 235.

[4] J. Appelbaum, *Sol Energy, 27* (1981) 421.

[5] P. Longrigg, *Sol. Cells, 13* (1985) 231.

[6] D. Jones, *J. Power Conversion Intelligent Motion, 15* (1989) 40.

[7] P.J Lawrenson, J M. Stephenson, P.T Blenkingsop, J. Corda and N.N Fulton, *Proc. Inst. Electr. Eng, Part B., 127* (1981) 253–265.

[8] P J. Lawrenson, W.F. Ray, R.M. Davis, J.M. Stephenson, N.N. Fulton and R.J. Blake, *Proc. First European Conf. Electrical Drives/Motors/Controls, Leeds, UK, 29 June–1 July, 1982,* pp. 23–31.

[9] R.M. Davis, W.F. Ray and R.J. Blake, *Proc Inst Electr Eng., Part B, 128* (1981) 126–136.

[10] J.W. Finch, M.R. Harris, H.M.B. Metwally and A. Musoke, *Proc. 2nd Int Conf. Electrical Machines – Design and Applications, London, UK, Sept. 1985,* pp. 134–138

[11] W.R Anis, *Sol. Cells, 28* (1990) 19

[12] H.M B. Metwally, Multi-tooth per pole variable reluctance motors, *Ph.D Thesis,* University of Newcastle upon Tyne, UK, May 1986.

[13] I. Karassik, W. Krutzsch, W Faser and J. Messina, *Pump Handbook,* McGraw-Hill, New York, *2nd edn,* 1986